Crystal Structures and Solution Behavior of Paramagnetic Divalent Transition Metal Complexes (Fe, Co) of the Sterically Encumbered Tridentate Macrocycles 1,4,7-R_3-1,4,7-Triazacyclononane: Coordination Numbers 5 (R = *i*-Pr) and 6 (R = *i*-Bu)

Alain Diebold, Abdelaziz Elbouadili, and Karl S. Hagen*

Department of Chemistry, Emory University, Atlanta, Georgia 30322

Received April 26, 2000

The coordination chemistry of the sterically hindered macrocyclic triamines, 1,4,7-R_3-1,4,7-triazacyclononane (R = *i*-Pr, *i*-Pr_3tacn, and R = *i*-Bu, *i*-Bu_3tacn) with divalent transition metals has been investigated. These ligands form a series of stable novel complexes with the triflate salts $M^{II}(CF_3SO_3)_2$ (M = Fe, Co, or Zn) under anaerobic conditions. The complexes Fe(*i*-Pr_3tacn)$(CF_3SO_3)_2$ (**2**), [Co(*i*-Pr_3tacn)$(SO_3CF_3)(H_2O)$](CF_3SO_3) (**3**), [Co(*i*-Pr_3tacn)$(CH_3CN)_2$]$(BPh_4)_2$ (**4**), Zn(*i*-Pr_3tacn)$(CF_3SO_3)_2$ (**5**), [Fe(*i*-Bu_3tacn)$(CH_3CN)_2(CF_3SO_3)$](CF_3SO_3) (**6**), Fe(*i*-Bu_3tacn)-$(H_2O)(CF_3SO_3)_2$ (**7**), and Co(*i*-Bu_3tacn)$(CF_3SO_3)_2$ (**8**) have been isolated. The behavior of these paramagnetic complexes in solution is explored by their ^{1}H NMR spectra. The solid-state structures of four complexes have been determined by X-ray single-crystal crystallography. Crystallographic parameters are as follows. **2**: $C_{17}H_{33}F_6FeN_3O_6S_2$, monoclinic, $P2_1/n$, a = 10.895(1) Å, b = 14.669(1) Å, c = 16.617(1) Å, β = 101.37(1)°, Z = 4. **3**: $C_{17}H_{35}CoF_6N_3O_7S_2$, monoclinic, $P2_1/c$, a = 8.669(2) Å, b = 25.538(3) Å, c = 12.4349(12) Å, β = 103.132(13)°, Z = 4. **6**: $C_{24}H_{45}F_6FeN_5O_6S_2$, monoclinic, $P2_1/c$, a = 12.953(6) Å, b = 16.780(6) Å, c = 15.790(5) Å, β = 96.32(2)°, Z = 4. **7**: $C_{20}H_{41}F_6FeN_3O_7S_2$, monoclinic, $C2/c$, a = 22.990(2) Å, b = 15.768(2) Å, c = 17.564(2) Å, β = 107.65(1)°, Z = 8. The ligand *i*-Pr_3tacn leads to complexes in which the metal ions are five-coordinate, while it's isobutyl homologue affords six-coordinate complexes. This difference in the stereochemistries around the metal center is attributed to steric interactions involving the bulky alkyl appendages of the macrocycles.

Introduction

Accurate synthetic models of some metalloproteins, in which the metal sites in at least some of the biologically relevant electronic states have intrinsic stability, can be synthesized using simple ligands.[1−3] Others, in which the protein environment of the metal dictates the structural, electronic, and/or chemical properties of the metal site, require more elaborate ligands to mimic the protein influences. Multidentate and macrocyclic ligands have been widely used in bioinorganic chemistry in recent years[4−6] for manipulating the geometries and the coordination numbers of the metal ions and, consequently, for controling the electronic structures and the reactivity of the metal complexes they form.

The first good structural models of the diiron(III) form of the non-heme protein hemerythrin (Hr) incorporated the tridentate azamacrocycles 1,4,7-triazacyclononane (tacn)[7,8] and tri-1-pyrazolylborate (Tp).[9,10] The tendency of these strong, facially coordinating ligands to form low-spin sandwich complexes with iron(II)[11] prevented their use in models of the diiron(II) form of Hr. However, the *N*-methylated derivative, 1,4,7-trimethyl-1,4,7-triazacyclononane (Me_3tacn), destabilizes the sandwich complex sufficiently such that the diiron(II) model complex could be isolated.[8,12] The methyl derivatives of Tp and Tp^{Me2} [13] and even the phenyl derivatives of Tp^{Ph} [14] formed sandwich complexes. It was not until the introduction of the steric constraints of the isopropyl groups in Tp^{i-Pr2} [15−18] that non-sandwich mononuclear and dinuclear iron(II) complexes could be made with tripodal ligands of this type.

In contrast, sterically hindered triazacyclononanes containing innocent substituents have been used less extensively in coordination chemistry. Sessler and co-workers have investigated the coordination of iron(III) to two sterically encumbered macrocycles, 1,4,7-triisopropyl-1,4,7-triazacyclononane (*i*-Pr_3-

(1) Ibers, J. A.; Holm, R. H. *Science* **1980**, *209*, 223−235.
(2) Karlin, K. D. *Science* **1993**, *261*, 701−708.
(3) Beinert, H.; Holm, R. H.; Munck, E. *Science* **1997**, *277*, 653−659.
(4) Wieghardt, K. *Angew. Chem., Int. Ed. Engl.* **1989**, *28*, 1153−1172.
(5) Lippard, S. J. *Angew. Chem., Int. Ed. Engl.* **1988**, *27*, 344−361.
(6) Bhula, R.; Osvath, P.; Weatherburn, D. C. *Coord. Chem. Rev.* **1988**, *91*, 89−213.
(7) Wieghardt, K.; Pohl, K.; Gebert, W. *Angew. Chem., Int. Ed. Engl.* **1983**, *22*, 727.
(8) Hartman, J. R.; Rardin, R. L.; Chaudhuri, P.; Pohl, K.; Wieghardt, K.; Nuber, B.; Weiss, J.; Papaefthymiou, G. C.; Frankel, R. B.; Lippard, S. J. *J. Am. Chem. Soc.* **1987**, *109*, 7387−7396.
(9) Armstrong, W. H.; Lippard, S. J. *J. Am. Chem. Soc.* **1983**, *105*, 4837−4838.
(10) Armstrong, W. H.; Spool, A.; Papaefthymiou, G. C.; Frankel, R. B.; Lippard, S. J. *J. Am. Chem. Soc.* **1984**, *106*, 3653−3667.
(11) Chaudhuri, P.; Wieghardt, K. *Prog. Inorg. Chem.* **1987**, *35*, 329−436.
(12) Chaudhuri, P.; Wieghardt, K.; Nuber, B.; Weiss, J. *Angew. Chem., Int. Ed. Engl.* **1985**, *24*, 778−779.
(13) Jesson, J. P.; Trofimenko, S.; Eaton, D. R. *J. Am. Chem. Soc.* **1967**, *89*, 3158−3164.
(14) Eichhorn, D. M.; Armstrong, W. H. *Inorg. Chem.* **1990**, *29*, 3607−3612.
(15) Kitajima, N.; Fukui, H.; Moro-oka, Y.; Mizutani, Y.; Kitagawa, T. *J. Am. Chem. Soc.* **1990**, *112*, 6402−6403.
(16) Kitajima, N.; Tamura, N.; Tanaka, M.; Moro-oka, Y. *Inorg. Chem.* **1992**, *31*, 3342−3343.
(17) Kitajima, N.; Amagai, H.; Tamura, N.; Ito, M.; Moro-oka, Y.; Heerwegh, K.; Penicaud, A.; Mathur, R.; Reed, C. A.; Boyd, P. D. W. *Inorg. Chem.* **1993**, *32*, 3583−3584.
(18) Kitajima, N.; Tamura, N.; Amagai, H.; Fukui, H.; Moro-oka, Y.; Mizutani, Y.; Kitagawa, T.; Mathur, R.; Heerwegh, K.; Reed, C. A.; Randall, C. R.; Que, L., Jr.; Tatsumi, K. *J. Am. Chem. Soc.* **1994**, *116*, 9071−9085.

10.1021/ic000456h CCC: $19.00
Published on Web 08/03/2000

tacn) and 1,4,7-triisobutyl-1,4,7-triazacyclononane (*i*-Bu_3tacn),[19] but these reactions did not result in complex formation in methanol. Instead, the singly protonated macrocycles acted as counterions to $[FeCl_4]^-$ and $[Fe_2OCl_6]^{2-}$ anions. The reduced affinity of these ligands for the iron(III) ion was attributed to steric interactions from the presence of the bulky isopropyl or isobutyl appendages. However, several vanadium, chromium, molybdenum, tungsten,[20−23] and titanium[24] complexes containing the ligand *i*-Pr_3tacn have been characterized.

More recently, the sterically hindered macrocycles *i*-Pr_3tacn and 1,4,7-tribenzyl-1,4,7-triazacyclononane (Bn_3tacn) have been used very effectively in copper coordination chemistry as part of synthetic modeling studies of copper-containing proteins.[25−32] The divergent steric and/or electronic properties of the ligands result in different reactivities of the *i*-Pr_3tacn and Bn_3tacn copper complexes.

In light of these observations, there is reason to believe that these ligands may form divalent metal complexes with properties different than those of their less sterically hindered derivatives, tacn and Me_3tacn. In addition, the alkyl substituents borne by these molecules render the complexes quite soluble in many polar and nonpolar organic solvents. Herein, we describe the synthesis and ligating properties of the sterically hindered triazacyclononanes *i*-Pr_3tacn and *i*-Bu_3tacn toward iron(II), cobalt(II), and zinc(II). We also report the structural characterization of four novel complexes as well as their associated spectroscopic properties.

Experimental Section

Materials and Physical Measurements. Reagents used were of commercially available reagent quality unless otherwise stated. All solvents were dried over appropriate reagents and distilled prior to use. Deoxygenation of solvents was effected by bubbling N_2 directly through the solutions. Preparation and handling of air-sensitive materials were performed under an inert atmosphere of N_2 in a glovebox. $M(CF_3SO_3)_2 \cdot 2CH_3CN$ (M = Fe, Co, or Zn) was prepared by reacting Fe, Co, or Zn metal with triflic acid in acetonitrile, and the product was crystallized by adding diethyl ether. The acetonitrile molecules in these salts are readily replaced with water when exposed to a humid atmosphere.[33] 1,4,7-Triazacyclononane (tacn) and 1,4,7-triisopropyl-1,4,7-triazacyclononane (*i*-Pr_3tacn) were synthesized according to literature procedures.[20−23,34] Elemental analyses were performed at Atlantic Microlabs, Inc., Atlanta, GA. ^{1}H NMR spectra were recorded on either the General Electric QE−300, the GE GN-500, or the Varian Inova 400 NMR spectrometer, using deuterated solvents as locks and referenced to tetramethylsilane. Electronic absorption spectra were collected on a Shimadzu UV-3101PC UV−vis−NIR scanning spectrophotometer.

1,4,7-Triisobutyl-1,4,7-triazacyclononane (*i*-Bu_3tacn). This tridentate macrocycle has been synthesized via a different route from that previously reported.[19] Isobutyryl chloride (2.7 mL, 25.8 mmol) was added dropwise at room temperature to a stirred solution containing tacn (1.0 g, 7.74 mmol) and triethylamine (6.5 mL, 46.6 mmol) in distilled CH_2Cl_2 (100 mL). The solution was left to stir overnight under a dinitrogen atmosphere and then washed with water (3 × 30 mL); the organic layer was dried over anhydrous $MgSO_4$, and the CH_2Cl_2 was removed with a rotary evaporator to give a brown solid residue. Column chromatography on silica with CH_2Cl_2 removed unreacted isobutyryl chloride. The intermediate 1,4,7-tri(isopropylcarbonyl)-1,4,7-triazacyclononane (2.37 g, 90%) was obtained as a pale yellow solid by using 9:1 CH_2Cl_2/CH_3OH as the eluent. ^{1}H NMR ($CDCl_3$, 300 MHz): δ 1.09 (d, J = 6.6 Hz, 18H, CH_3), 2.70 (septet, J = 6.6 Hz, 3H, CH), 3.40 (t, J = 4.3 Hz, 6H, CH_2), 3.70 (t, J = 4.3 Hz, 6H, CH_2).

The triamide (2.37 g, 6.98 mmol) was dissolved in dry THF (50 mL); a solution of BH_3·THF (80 mL, 80 mmol) was added, and the mixture was refluxed overnight under a dinitrogen atmosphere. After being cooled to room temperature, the excess BH_3·THF was quenched by slow addition of methanol, and the colorless solution was evaporated to leave a colorless oil. This was dissolved in 1-butanol (50 mL), water (50 mL), and concentrated HCl (80 mL) and refluxed overnight. After the mixture was cooled, sodium hydroxide was added until pH ≥12, and the product was extracted with CH_2Cl_2 (6 × 50 mL). The combined CH_2Cl_2 extracts were dried over $MgSO_4$ and evaporated to give 1.91 g (92%) of the title compound as a pale yellow oil. ^{1}H NMR ($CDCl_3$, 300 MHz): δ 0.90 (d, J = 6.6 Hz, 18H, CH_3), 1.67 (m, 3H, CH), 2.21 (d, J = 7.2 Hz, 6H, $CH_{2(i-Bu)}$), 2.72 (s, 12H, $CH_{2(tacn)}$).

(*i*-Pr_3tacnH)$^+$(Me_3CCO_2)$^-$ (1). A colorless solution of pivalic acid (51 mg, 0.5 mmol) in CH_3CN (1 mL) was added to a solution of *i*-Pr_3tacn (0.13 g, 0.5 mmol) in CH_3CN (2 mL), leading to a clear, pale yellow solution. The reaction mixture was stirred for 30 min at room temperature, and the solvent was removed under vacuum, affording the title compound as a pale yellow gummy residue. ^{1}H NMR (CD_3CN, 300 MHz): δ 1.13 (d, 18H, $CH_{3(i-Pr)}$), 2.21 (s, 9H, $CH_{3(Me3C)}$), 2.60 (m, 6H, CH_2), 2.90 (m, 6H, CH_2), 3.12 (m, 3H, CH), 10.12 (br s, 1H, NH^+). The perchlorate salt was prepared as previously reported[20a] to obtain its NMR spectrum for comparison. ^{1}H NMR for (*i*-Pr_3tacnH)$^+$(ClO_4)$^-$ (CD_3CN, 400 MHz): δ 1.13 (d, 18H, $CH_{3(i-Pr)}$), 2.60 (m, 6H, CH_2), 2.80 (m, 6H, CH_2), 3.12 (m, 3H, CH), 10.0 (s, 1H, NH^+).

Fe^{II}(*i*-Pr_3tacn)(CF_3SO_3)$_2$ (2). A colorless solution of $Fe(CF_3SO_3)_2 \cdot 2CH_3CN$ (0.44 g, 1.0 mmol) in CH_3CN (2 mL) was added to a solution of *i*-Pr_3tacn (0.26 g, 1.0 mmol) in CH_3CN (2 mL), affording a clear, light-green solution. The reaction mixture was stirred for 30 min at room temperature, and the solvent was removed under vacuum. Colorless crystals of **2** suitable for X-ray diffraction analysis were grown at ambient temperature by slow diffusion of pentane into a dilute $CHCl_3$ solution of **2**. The colorless crystals were removed by filtration and dried under vacuum, yielding 186 mg (31%) of the title complex as a white solid. ^{1}H NMR (CD_2Cl_2, 300 MHz): δ −28.3 (CH_3), −2.9 (CH), 17.8 (CH_2), 74.3 (CH_2), 98.6 (CH_2), 195.6 (CH_2). ^{1}H NMR (CD_3CN, 400 MHz): δ −2.3 (br s, 18H, CH_3), 21.6 (br s, 3H, CH), 51.1 (br s, 6H, CH_2). Anal. Calcd for $C_{17}H_{33}N_3F_6FeO_6S_2$: C, 33.50; H, 5.46; N, 6.89. Found: C, 33.4; H, 5.4; N, 6.9.

[Co^{II}(*i*-Pr_3tacn)(CF_3SO_3)(H_2O)](CF_3SO_3) (3). A pink suspension of $Co(CF_3SO_3)_2 \cdot 2H_2O$ (0.39 g, 1.0 mmol) in CH_3CN (2 mL) was added to a solution of *i*-Pr_3tacn (0.26 g, 1.0 mmol) in CH_3CN (2 mL), affording a clear, dark-purple solution. The reaction mixture was stirred for 30 min at room temperature, and the solvent was removed under vacuum. Purple crystals of **3** suitable for X-ray diffraction analysis were grown at ambient temperature by slow diffusion of pentane into a dilute acetone solution of **3**. The purple crystals were removed by filtration and dried under vacuum, yielding 327 mg (52%) of the title complex. ^{1}H NMR

(19) Sessler, J. L.; Sibert, J. W.; Lynch, V. *Inorg. Chim. Acta* **1994**, *216*, 89−95.
(20) Haselhorst, G.; Stoetzel, S.; Strassburger, A.; Walz, W.; Wieghardt, K.; Nuber, B. *J. Chem. Soc., Dalton Trans.* **1993**, 83−90.
(21) Stoetzel, S.; Wieghardt, K.; Nuber, B. *Inorg. Chem.* **1993**, *32*, 2128−2131.
(22) Böhmer, J.; Haselhorst, G.; Wieghardt, K.; Nuber, B. *Angew. Chem., Int. Ed. Engl.* **1994**, *33*, 1473−1476.
(23) Böhmer, J.; Wieghardt, K.; Nuber, B. *Angew. Chem., Int. Ed. Engl.* **1995**, *34*, 1435−1437.
(24) Jeske, P.; Wieghardt, K.; Nuber, B. *Inorg. Chem.* **1994**, *33*, 47−53.
(25) Mahapatra, S.; Halfen, J. A.; Wilkinson, E. C.; Que, L., Jr.; Tolman, W. B. *J. Am. Chem. Soc.* **1994**, *116*, 9785−9786.
(26) Mahapatra, S.; Halfen, J. A.; Wilkinson, E. C.; Pan, G.; Cramer, C. J.; Que, L., Jr.; Tolman, W. B. *J. Am. Chem. Soc.* **1995**, *117*, 8865−8866.
(27) Halfen, J. A.; Tolman, W. B. *J. Am. Chem. Soc.* **1994**, *116*, 5475−5476.
(28) Halfen, J. A.; Mahapatra, S.; Olmstead, M. M.; Tolman, W. B. *J. Am. Chem. Soc.* **1994**, *116*, 2173−2174.
(29) Halfen, J. A.; Mahapatra, S.; Wilkinson, E. C.; Gengenbach, A. J.; Young, V. G., Jr.; Que, L., Jr.; Tolman, W. B. *J. Am. Chem. Soc.* **1996**, *118*, 763−776.
(30) Schneider, J. L.; Young, V. G. J.; Tolman, W. B. *Inorg. Chem.* **1996**, *35*, 5410−5411.
(31) Tolman, W. B. *Adv. Chem. Ser.* **1995**, *246*, 195−217.
(32) Tolman, W. B. *Acc. Chem. Res.* **1997**, *30*, 227−237.
(33) Hagen, K. S. *Inorg. Chem.*, in press.
(34) Wieghardt, K.; Schmidt, W.; Nuber, B.; Weiss, J. *Chem. Ber.* **1979**, *112*, 2220−2230.

(CD_3CN, 300 MHz): δ −68.4 (br s, 3H, CH), −33.1 (br s, 18H, CH_3), 39.9 (br s, 6H, CH_2), 226.7 (br s, 6H, CH_2). ^1H NMR ($CDCl_3$, 300 MHz): δ −78.9 (br s, 3H, CH), −43.2 (br s, 18H, CH_3). Anal. Calcd for $C_{17}H_{35}N_3CoF_6O_7S_2$: C, 32.38; H, 5.60; N, 6.66. Found: C, 32.4; H, 5.5; N, 6.6. UV−vis (λ_{max}, nm (ϵ, M^{-1} cm^{-1}), 8.16×10^{-3} M in CH_3CN): 470 (26), 525 (32), 652 (11). UV−vis (λ_{max}, nm (ϵ, M^{-1} cm^{-1}), 8.16×10^{-3} M in $CHCl_3$): 468 (17), 560 (20), 700 (6).

$[Co^{II}(i\text{-}Pr_3tacn)(CH_3CN)_2](BPh_4)_2$ (4). All the dark purple solid from a crude sample of **3** prepared on a 1.0 mmol scale in CH_3CN, as described above, was dissolved in dry CH_3OH (3 mL), yielding a pink solution. A solution of $NaBPh_4$ (689 mg, 2.0 mmol) in CH_3OH (5 mL) was slowly added. A pale pink precipitate appeared immediately, which was filtered off and washed with CH_3OH. Drying in vacuo yielded 787 mg (83%) of a light-pink powder. ^1H NMR (CD_3CN, 300 MHz): δ −69.4 (br s, 3H, CH), −31.3 (br s, 18H, CH_3), 7.4 (s, 8H, BPh_4^-), 7.7 (s, 16H, BPh_4^-), 8.4 (s, 16H, BPh_4^-), 65.4 (br s, 6H, CH_2), 232.7 (br s, 6H, CH_2). Anal. Calcd for $C_{47}H_{79}B_2CoN_5\cdot(CH_3OH)_{1.5}$: C, 75.97; H, 7.91; N, 6.47. Found: C, 76.0; H, 7.9; N, 6.5. UV−vis (λ_{max}, nm (ϵ, M^{-1} cm^{-1}), 5.25×10^{-3} M in CH_3CN): 464 (30), 530 (34), 671 (14). UV−vis (λ_{max}, nm (ϵ, M^{-1} cm^{-1}), 5.25×10^{-3} M in acetone): 452 (27), 548 (24), 703 (9). IR (KBr, cm^{-1}): ν_{CN} = 2300 and 2271.

$Zn^{II}(i\text{-}Pr_3tacn)(CF_3SO_3)_2$ (5). A suspension of $Zn(CF_3SO_3)_2\cdot 2CH_3CN$ (0.45 g, 1.0 mmol) in CH_3CN (2 mL) was added to a solution of *i*-Pr_3tacn (0.26 g, 1.0 mmol) in CH_3CN (2 mL), yielding a clear, colorless solution. The reaction mixture was stirred for 30 min at room temperature, and the solvent was removed under vacuum, leading to a light yellow residue. This residue was dissolved in CH_2Cl_2, and precipitation with pentane afforded 549 mg (89%) of a light-yellow powder. ^1H NMR (CD_3CN, 300 MHz): δ 1.18 (br s, 18H, CH_3), 2.74 (br m, 6H, CH_2), 2.91 (br m, 6H, CH_2), 3.35 (br m, 3H, CH). Anal. Calcd for $C_{17}H_{33}F_6O_6S_2Zn(CH_2Cl_2)_{1.3}$: C, 30.14; H, 4.92; N, 5.76. Found: C, 30.0; H, 5.2; N, 5.8.

$[Fe^{II}(i\text{-}Bu_3tacn)(CH_3CN)_2(CF_3SO_3)](CF_3SO_3)$ (6). A colorless solution of $Fe(CF_3SO_3)_2\cdot 2CH_3CN$ (0.44 g, 1.0 mmol) in CH_3CN (2 mL) was added to a solution of *i*-Bu_3tacn (0.30 g, 1.0 mmol) in CH_3CN (2 mL), affording a clear, yellow-light-brown solution. The reaction mixture was stirred for 30 min at room temperature, and the solvent was removed under vacuum. Colorless crystals of **6** suitable for X-ray diffraction analysis were grown at −30 °C by slow diffusion of heptane into a dilute $CH_3CN/CHCl_3$ solution of **6**. The colorless crystals were removed by filtration and dried under vacuum, yielding 270 mg (38%) of the title complex as a white solid. ^1H NMR (CD_3CN, 400 MHz): δ −8.1 (br s, 3H, CH), −1.8 (br s, 18H, CH_3), 48.3 (br s, 6H, $CH_{2(tacn)}$), 113.5 (br s, 6H, $CH_{2(tacn)}$). Anal. Calcd for $C_{20}H_{39}F_6FeN_3O_6S_2\cdot(CHCl_3)_{0.5}$: C, 34.62; H, 5.60; N, 5.91. Found: C, 34.6; H, 5.6; N, 5.9.

$Fe^{II}(i\text{-}Bu_3tacn)(H_2O)(CF_3SO_3)_2$ (7). A 71 mg (0.1 mmol) sample of the white solid of **6** from the 1.0 mmol scale preparation was dissolved in $CHCl_3$ (2 mL), yielding a colorless solution. A 1.8 μL (0.1 mmol) sample of H_2O was added, and the reaction mixture was stirred for 30 min at room temperature. After a few minutes, colorless needles precipitated out, which were filtered off and washed with cold $CHCl_3$. Drying under vacuum yielded 56 mg (84%) of the title compound as a white powder. Colorless crystals of **7** suitable for X-ray diffraction analysis were grown by slow diffusion of pentane into a $CHCl_3$ solution of **7**. ^1H NMR ($(CD_3)_2CO$, 300 MHz): δ −13.2 (br s, 3H, CH), −4.5 (br s, 18H, CH_3), 42.9 (br s, 6H, $CH_{2(tacn)}$), 133.3 (br s, 6H, $CH_{2(tacn)}$). ^1H NMR (CD_3CN, 400 MHz): δ −8.1 (br s, 3H, CH), −1.8 (br s, 18H, CH_3), 48.3 (br s, 6H, $CH_{2(tacn)}$), 113.5 (br s, 6H, $CH_{2(tacn)}$). Anal. Calcd for $C_{20}H_{41}N_3F_6FeO_7S_2$: C, 35.88; H, 6.17; N, 6.28. Found: C, 36.2; H, 6.1; N, 6.2.

$Co^{II}(i\text{-}Bu_3tacn)(CF_3SO_3)_2$ (8). A colorless solution of *i*-Bu_3tacn (0.30 g, 1.0 mmol) in CH_3CN (2 mL) was added to a pink solution of $Co(CF_3SO_3)_2\cdot 2CH_3CN$ (0.44 g, 1.0 mmol) in CH_3CN (4 mL), affording a dark-purple reaction mixture. This solution was stirred for 30 min at ambient temperature, and the solvent was removed under vacuum, yielding a pink gummy residue. Orange needles of **8** were obtained at −30 °C by slow diffusion of ether into a dilute CH_3CN solution of **8**. The needles were removed by filtration and dried under vacuum, yielding 346 mg (53%) of the title complex as a pink solid. ^1H NMR (CD_3CN, 300 MHz): δ −47.8 (br s, 6H, $CH_{2(i-Bu)}$), −19.3 (br s, 3H, CH), −10.4 (br s, 18H, CH_3), 39.5 (br s, 6H, $CH_{2(tacn)}$), 191.2 (br s, 6H, $CH_{2(tacn)}$). Anal. Calcd for $C_{20}H_{39}N_3CoF_6O_6S_2$: C, 36.70; H, 6.01; N, 6.42. Found: C, 36.5; H, 6.2; N, 6.2. UV−vis (λ_{max}, nm (ϵ, M^{-1} cm^{-1}), 7.64×10^{-3} M in CH_3CN): 470 (32), 1027 (8). UV−vis (λ_{max}, nm (ϵ, M^{-1} cm^{-1}), 7.64×10^{-3} M in $CHCl_3$): 486 (14), 1200 (7).

Crystallographic Studies. Crystals of **2**, **3**, **6**, and **7** suitable for X-ray crystallographic analysis were obtained as described in Experimental Section (vide supra). All crystals were coated with a viscous oil and mounted with super glue on the end of a glass fiber. The diffraction intensities were collected using Mo Kα graphite-monochromated radiation (λ = 0.710 73 Å) on a Siemens P4 single-crystal X-ray diffractometer (**2**) or on a Siemens P4/RA single-crystal X-ray diffractometer with Cu Kα graphite-monochromated radiation (λ = 1.541 78 Å) (**3**, **6**, and **7**). During data collection, the intensities of three representative reflections were monitored every 97 reflections and indicated decays of 5% (**2**), 12% (**3**), 6% (**6**), and 18% (**7**). The structures were solved either by direct methods or by Patterson interpretation and expansion (SHELXS-86) and difference Fourier methods, and they were refined by full-matrix least-squares methods (SHELXTL). All atoms in the coordination sphere were refined with anisotropic thermal parameters. Hydrogen atoms were included and placed at calculated positions with C−H bond distances fixed at 0.96 Å—except for complex **7**, in which the hydrogen atoms of the water molecule were located from the difference Fourier map—and their positions refined. The details of the data collection and refinement procedures are given in Table 1 and in the Supporting Information. Selected bond lengths and angles are given in Tables 2 and 3.

Results and Discussion

Ligand Synthesis. The two triazamacrocycles tacn and *i*-Pr_3tacn were synthesized following procedures described by Wieghardt and co-workers.[20−23,34] Direct alkylation of the secondary amino groups of azamacrocycles with simple aliphatic alkyl halides such as isobutyl chloride could lead to quaternization of the N atoms, producing species with no metal-ligating properties. To overcome this problem, the two-step reaction sequence similar to that reported by Moore and co-workers[35] for *N*-alkylated cyclam was adopted. The macrocycle *i*-Bu_3tacn was produced in 83% yield based on tacn by the reaction of isobutyryl chloride with tacn in the presence of triethylamine, followed by the reduction of the resulting triamide with $BH_3\cdot$THF. Unlike tacn, the alkylated ligands, R_3tacn (R = Me, *i*-Pr, *i*-Bu, or CH_2Ph), are free-flowing liquids or oils at room temperature. This physical property is reflective of the presence of the three alkyl substituents on the nitrogen atoms of the macrocycle that effectively reduce intermolecular interactions.

Synthesis of Complexes. A variety of complexes can be prepared from the reaction of the corresponding ligand (*i*-Pr_3tacn or *i*-Bu_3tacn) with divalent transition metal triflate salts, $M^{II}(CF_3SO_3)_2$ (M = Fe, C, or Zn), under anaerobic conditions (Scheme 1). The metal triflates are particularly useful reagents, as they can be easily prepared in a soluble, solvated form from the corresponding metal powder and triflic acid in a variety of solvents.[33] They are air stable, can easily be made anhydrous, contain a weakly coordinating anion, and are a safe substitute for the perchlorate salts.

Direct addition of pivalic acid to *i*-Pr_3tacn in acetonitrile affords the monoprotonated form of the tri-*N*-substituted macrocycle as the pivalate salt. This species exhibits ^1H NMR features identical to those observed for the monohydroperchlorate salt, with the exception of the broad peak corresponding to the pivalate anion.

The complexes $Fe(i\text{-}Pr_3tacn)(CF_3SO_3)_2$ (**2**), $[Co(i\text{-}Pr_3tacn)(CF_3SO_3)(H_2O)](CF_3SO_3)$ (**3**), and $Zn(i\text{-}Pr_3tacn)(CF_3SO_3)_2$ (**5**)

(35) Alcock, N. W.; Benniston, A. C.; Grant, S. J.; Omar, H. A. A.; Moore, P. *J. Chem. Soc., Chem. Commun.* **1991**, 1573−1575.

Scheme 1

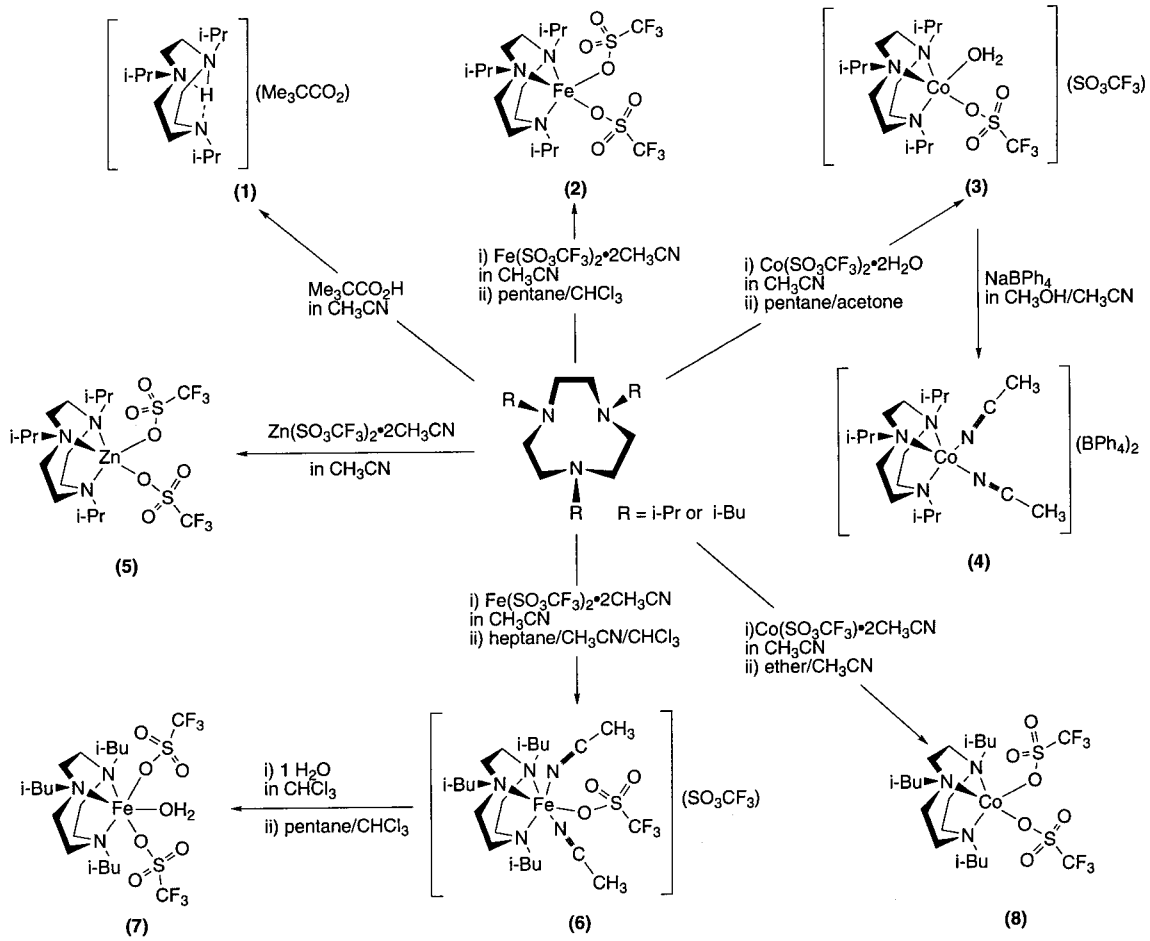

were prepared by the reaction of the respective divalent transition metal triflate salt $M^{II}(CF_3SO_3)_2$ and the ligand *i*-Pr_3tacn (1:1) in acetonitrile under a dinitrogen atmosphere. The five-coordinate iron(II) complex (**2**), in which the two triflate anions are bound, can be crystallized in low yield (31%) as colorless crystals from a pale-gray-green oil that forms in chloroform. The low yield obtained was a consequence of complex **2** forming together with other species which have not been identified and/or of complex **2** existing as an equilibrium mixture in solution. Purple crystals of the corresponding five-coordinate cobalt(II) complex, **3**, were obtained in a satisfactory yield (52%) by slow diffusion of pentane into an acetone solution. An X-ray crystal structure study revealed the presence of a terminal water molecule as well as one triflate anion coordinated to the cobalt. The second triflate remains uncoordinated. Pale-orange crystals not suitable for an X-ray diffraction analysis were isolated from solutions of **3** in a coordinating solvent such as acetonitrile. The observed color change presumably indicates the presence of at least one acetonitrile ligand in the coordination sphere. This transformation is easily reversed by application of a vacuum, leading to the loss of the coordinated acetonitrile ligands, and this transformation can also be monitored with a ^1H NMR experiment. Indeed, different spectra were observed in coordinating (CD_3CN) or noncoordinating ($CDCl_3$) solvents (vide infra). A pure, light-pink complex, $[Co^{II}(i\text{-}Pr_3\text{tacn})(CH_3CN)_2](BPh_4)_2$ (**4**), was isolated when 2 equiv of tetraphenylborate in methanol was added to an acetonitrile solution of **3**.

The white six-coordinate $[Fe(i\text{-}Bu_3\text{tacn})(CH_3CN)_2(CF_3SO_3)](CF_3SO_3)$ complex (**6**) was readily synthesized in acetonitrile by adding 1 equiv of $Fe(CF_3SO_3)_2\cdot 2CH_3CN$ to 1 equiv of *i*-Bu_3tacn under a dinitrogen atmosphere. The presence of the two terminal acetonitrile ligands was confirmed from an X-ray crystal structure study. The tetraphenylborate salt precipitated as a white solid that was insoluble in all common polar and nonpolar solvents. This precluded a single-crystal structure determination and characterization by NMR spectroscopy. The addition of 1 equiv of H_2O to **6** in solution in a noncoordinating solvent ($CHCl_3$) affords a new, less soluble iron(II) complex. The crystal structure reveals a six-coordinate aqua complex, $Fe(i\text{-}Bu_3\text{tacn})(H_2O)(CF_3SO_3)_2$ (**7**). An orange cobalt analogue of **6**, $[Co(i\text{-}Bu_3\text{tacn})(CH_3CN)_x](CF_3SO_3)_2$, was isolated from an acetonitrile solution containing $Co(CF_3SO_3)_2\cdot 2CH_3CN$ and *i*-Bu_3tacn. The coordinated acetonitrile molecules are readily lost under vacuum, leading to a pink complex that was analyzed as $Co(i\text{-}Bu_3\text{tacn})(CF_3SO_3)_2$ (**8**).

Solutions of **2**, **3**, **4**, **6**, **7**, and **8** are quite sensitive to dioxygen. This reactivity, which varies from complex to complex, will be the subject of a future report.

Crystal Structures of the Complexes. X-ray structures of four representative complexes have been determined to demonstrate the structural preferences of divalent first-row transition metal complexes containing the isopropyl- and isobutyl-substituted tacn ligands. The complexes all crystallize in centrosymmetric space groups as racemic mixtures of enantiomers containing the $\lambda\lambda\lambda$ and $\delta\delta\delta$ configurations of the three five-membered rings in the metal-bound tacn ligands. A summary of crystal parameters and refinement results of these complexes is given in Table 1, and selected bond distances and angles appear in Tables 2 and 3. The molecular structures of these complexes are shown in Figures 1−4.

Table 1. Crystallographic Data for the Complexes **2**, **3**, **6**, and **7**

	2	**3**	**6**	**7**
empirical formula	$C_{17}H_{33}F_6FeN_3O_6S_2$	$C_{17}H_{35}CoF_6N_3O_7S_2$	$C_{24}H_{45}F_6FeN_5O_6S_2$	$C_{20}H_{41}F_6FeN_3O_7S_2$
fw	609.43	630.53	733.62	669.53
T, °C	−100	−100	−100	−100
λ, Å	0.710 73 (Mo Kα)	1.541 78 (Cu Kα)	1.541 78 (Cu Kα)	1.541 78 (Cu Kα)
space group, No.	$P2_1/n$, 14	$P2_1/c$, 14	$P2_1/c$, 14	$C2/c$, 15
a, Å	10.895(1)	8.669(2)	12.953(6)	22.990(2)
b, Å	14.669(1)	25.538(3)	16.780(6)	15.768(2)
c, Å	16.617(1)	12.4349(12)	15.790(5)	17.564(2)
β, deg	101.37(1)	103.132(13)	96.32(2)	107.65(1)
V, Å^3	2603.6(3)	2681.1(8)	3411.1(23)	6067.3(12)
Z	4	4	4	8
ρ_{calcd}, g cm^{-3}	1.555	1.562	1.429	1.466
μ, cm^{-1}	8.19	72.40	53.71	59.86
R^a	0.0432	0.0740	0.0581	0.0794
$R_w{}^b$	0.1035	0.1897	0.1451	0.2074

^{a} $R = \Sigma||F_o| - |F_c||/\Sigma|F_o|$. ^{b} $R_w = [\Sigma w(F_o^2 - F_c^2)^2/\Sigma w(F_o^2)^2]^{1/2}$.

Table 2. Selected Bond Distances (Å) and Bond Angles (deg) for **2** and **3**

	2 (M = Fe)	**3** (M = Co)
M−N1	2.220(3)	2.153(6)
M−O1	2.125(2)	2.076(5)
M−N2	2.173(2)	2.077(6)
M−N3	2.149(3)	2.113(6)
M−O4	2.000(2)	2.058(5)
N1−M−O1	176.09(9)	178.4(2)
N1−M−N2	81.82(10)	86.5(2)
N1−M−N3	84.06(10)	82.6(2)
N1−M−O4	92.22(10)	91.4(2)
O1−M−N2	96.24(9)	94.8(2)
O1−M−N3	92.40(10)	98.3(2)
O1−M−O4	91.43(9)	87.2(2)
N2−M−N3	85.11(10)	87.6(2)
N2−M−O4	140.28(11)	120.9(2)
N3−M−O4	133.55(11)	150.6(2)

Table 3. Selected Bond Distances (Å) and Bond Angles (deg) for **6** and **7**

		6		**7**
Fe−N1		2.210(4)		2.225(6)
Fe−N2		2.198(4)		2.218(7)
Fe−N3		2.223(4)		2.217(6)
Fe−O1		2.093(3)		2.086(6)
Fe−L	N4	2.166(4)	O2	2.171(5)
	N5	2.157(4)	O5	2.095(5)
N1−Fe−N2		81.01(13)		81.5(2)
N1−Fe−N3		81.79(14)		81.6(2)
N1−Fe−O1		94.94(13)		96.0(2)
N1−Fe−L	N4	96.3(2)	O2	172.6(2)
N1−Fe−L	N5	174.43(13)	O5	96.0(2)
N2−Fe−N3		82.33(13)		81.5(2)
N2−Fe−O1		174.88(13)		176.0(2)
N2−Fe−L	N4	94.19(14)	O2	95.0(2)
N2−Fe−L	N5	93.73(13)	O5	92.4(2)
N3−Fe−O1		94.04(13)		95.0(2)
N3−Fe−L	N4	176.25(14)	O2	91.4(2)
N3−Fe−L	N5	95.77(14)	O5	173.7(2)
O1−Fe−L	N4	89.34(14)	O2	87.2(2)
O1−Fe−L	N5	90.22(13)	O5	91.0(2)
N4−Fe−N5		85.8(2)		
O2−Fe−O5				90.6(2)

Fe(*i*-Pr$_3$tacn)(CF$_3$SO$_3$)$_2$ (2). An ORTEP diagram of the structure is given in Figure 1. The asymmetric unit of this crystal structure contains a discrete mononuclear unit of the neutral complex **2**. In this compound, the coordination sphere about the five-coordinate iron(II) is a distorted trigonal bipyramid with ligation from the tertiary amines from the *i*-Pr$_3$tacn ligand and two triflate oxygens. The N−Fe−N angles average 84° to accommodate the five-membered chelate rings enforced by this

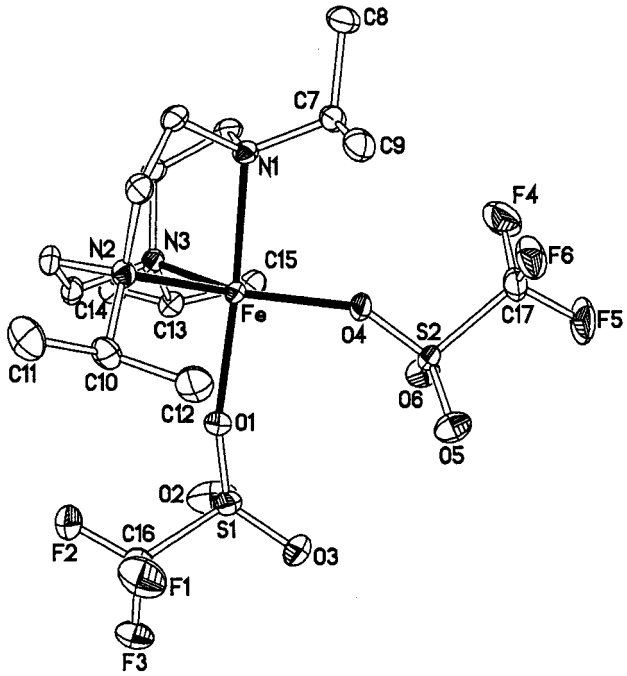

Figure 1. Molecular structure and atom-labeling scheme for Fe(*i*-Pr$_3$-tacn)(CF$_3$SO$_3$)$_2$ (**2**). All hydrogen atoms have been omitted for clarity. Thermal ellipsoids are at the 30% probability level.

tridentate macrocycle. The two axial positions are occupied by one *i*-Pr$_3$tacn nitrogen atom (N1) and one triflate anion oxygen atom (O1), resulting in asymmetry in the Fe−N and Fe−O distances. Indeed, the Fe−N1 distance (2.220(3) Å) is significantly longer than the two equatorial metal−nitrogen distances (2.173(2) and 2.149(3) Å for N2 and N3, respectively). The Fe−O distances are 2.125(2) Å for the axial triflate ligand and 2.000(2) Å for the equatorial triflate ligand. The N1−Fe−O1 angle (176.09(9)°) is nearly linear. The principal distortion from an idealized trigonal bipyramidal geometry is the intraligand (*i*-Pr$_3$tacn) N−Fe−N bond angle which is significantly smaller than those between the *i*-Pr$_3$tacn nitrogen atoms and the triflate oxygen atom (N2−Fe−N3 = 85.1(1)° vs N2−Fe−O4 = 140.3(1)° and N3−Fe−O4 = 133.6(1)°). The asymmetry in the equatorial N−Fe−O angles probably results from interactions between the CH group (C7) of the isopropyl substituent borne by the nitrogen atom N1 and the bound oxygen atom (O4) of the triflate (O4···C7 = 3.028 Å). The Fe−N distances range from 2.149(3) to 2.220(3) Å, which is characteristic of high-

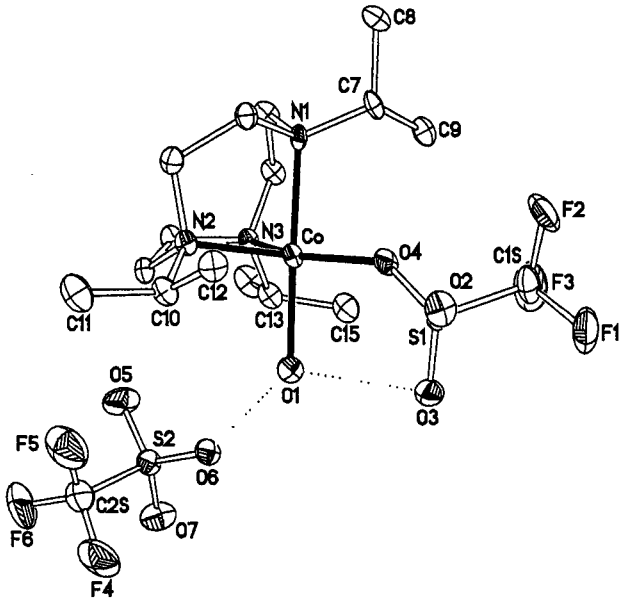

Figure 2. Molecular structure and atom-labeling scheme for [Co(*i*-Pr_3tacn)(CF_3SO_3)(H_2O)](CF_3SO_3) (**3**), illustrating hydrogen bonding. All hydrogen atoms have been omitted for clarity. Thermal ellipsoids are at the 30% probability level.

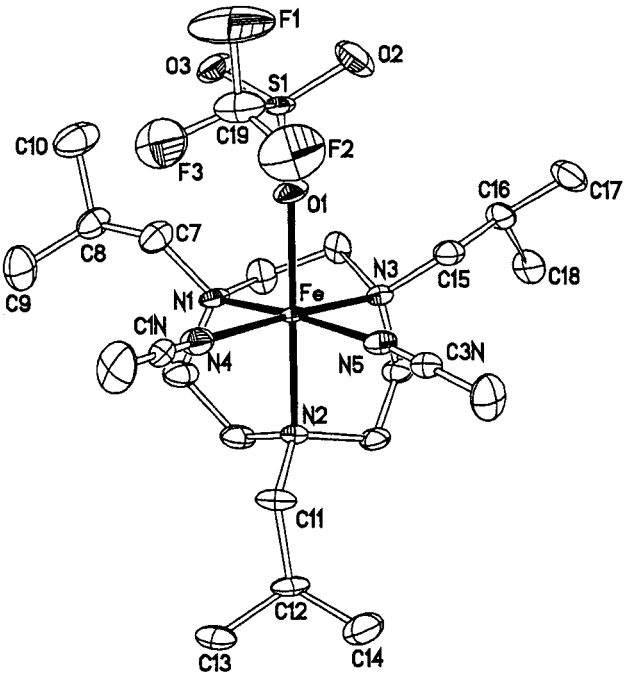

Figure 3. Molecular structure and atom-labeling scheme for [Fe(*i*-Bu_3tacn)(CH_3CN)$_2$(CF_3SO_3)]$^+$ (**6**). All hydrogen atoms have been omitted for clarity. Thermal ellipsoids are at the 50% probability level.

spin iron(II)[36] and indicates that the aliphatic amine nitrogens bind only weakly to the iron ion.

[Co(*i*-Pr_3tacn)(CF_3SO_3)(H_2O)](CF_3SO_3) (3). The structure of **3** is depicted in Figure 2. The complex is isomorphous with the analogous copper(II) complex that was reported recently.[27] Complex **3** consists of one cobalt(II) atom with the *i*-Pr_3tacn ligand coordinated in a tridentate fashion, one water molecule, and one terminally bonded triflate anion completing the coordination sphere. The second triflate ion is noncoordinated, but is linked by a hydrogen bond to the coordinated water. The

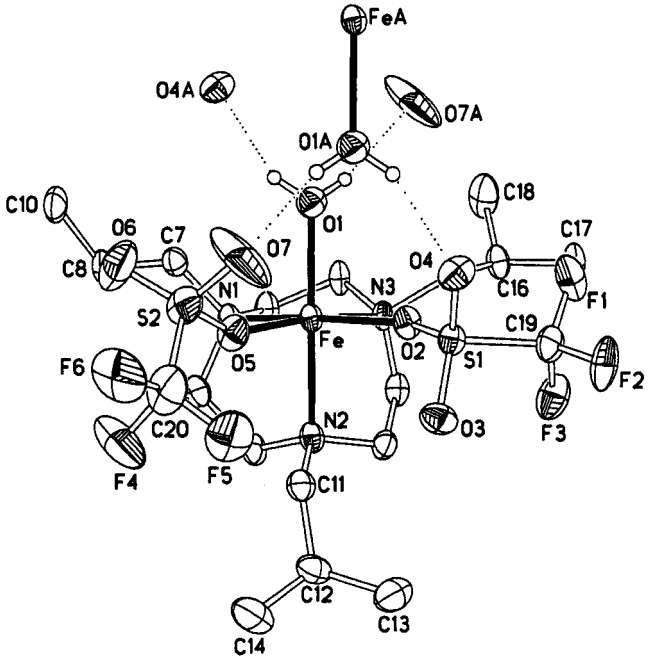

Figure 4. Molecular structure and atom-labeling scheme for Fe(*i*-Bu_3-tacn)(H_2O)(CF_3SO_3)$_2$ (**7**), illustrating intermolecular hydrogen bonding. All hydrogen atoms except those of the water molecule have been omitted for clarity. Thermal ellipsoids are at the 30% probability level.

geometry about the five-coordinate cobalt ion is distorted away from either a trigonal bipyramid or a square pyramid. If it is described as the former, one *i*-Pr_3tacn nitrogen atom (N1) and the aqua ligand oxygen atom (O1) occupy the axial positions. The Co−N1 distance (2.153(6) Å) is thereby significantly longer than the other two metal−nitrogen distances (average, 2.094 Å). The angle between the cobalt and the two axial positions is nearly linear (N1−Co−O1 = 178.4(2)°). The distortion from a trigonal bipyramidal geometry is particularly noticeable in the equatorial plane. Although the N2−Co−O4 angle (120.9(2)°) is close to the ideal value, large deviations are seen in the two other angles. The presence of the five-membered chelate ring, enforced by the characteristic configuration of this ligand, appears to be responsible for the acute N2−Co−N3 angle (87.6(2)°). On the other hand, the large N3−Co−O4 angle (150.6(2)°) may be most likely a consequence of interactions between the CH group (C7) of the isopropyl substituent borne by the nitrogen atom N1 and the coordinated oxygen atom (O4) of the monodentate triflate (O4···C7 = 2.993 Å). The water molecule is hydrogen bonded to both the coordinated and uncoordinated triflates, as indicated by the O1···O3 and O1···O6 distances of 2.861 and 2.705 Å, respectively (the water hydrogen atoms have been placed at calculated positions).

[Fe(*i*-Bu_3tacn)(CH_3CN)$_2$(CF_3SO_3)](CF_3SO_3) (6). The structure of the cation [Fe(*i*-Bu_3tacn)(CH_3CN)$_2$(CF_3SO_3)]$^+$ from **6** (Figure 3) shows a six-coordinate iron(II) complex with the *i*-Bu_3tacn ligand acting as a tridentate facial-coordinating ligand. The remaining coordination sites are occupied by two acetonitrile ligands and a terminally bonded triflate. The iron center is arranged in an approximate octahedral geometry with Fe−N distances ranging from 2.157(4) to 2.223(4) Å, which is typical of high-spin iron(II). Like the two previous complexes, the acute intraligand N−Fe−N bond angles (average, 81.7°) result from the presence of the five-membered chelate rings enforced by the *i*-Bu_3tacn ligand. The coordination of one acetonitrile molecule is nearly linear with an Fe−N5−C3N angle of 173.9(4)°, although the second molecule is bent (Fe−N4−C1N

(36) Butcher, R. J.; Addison, A. W. *Inorg. Chim. Acta* **1989**, *158*, 211−215.

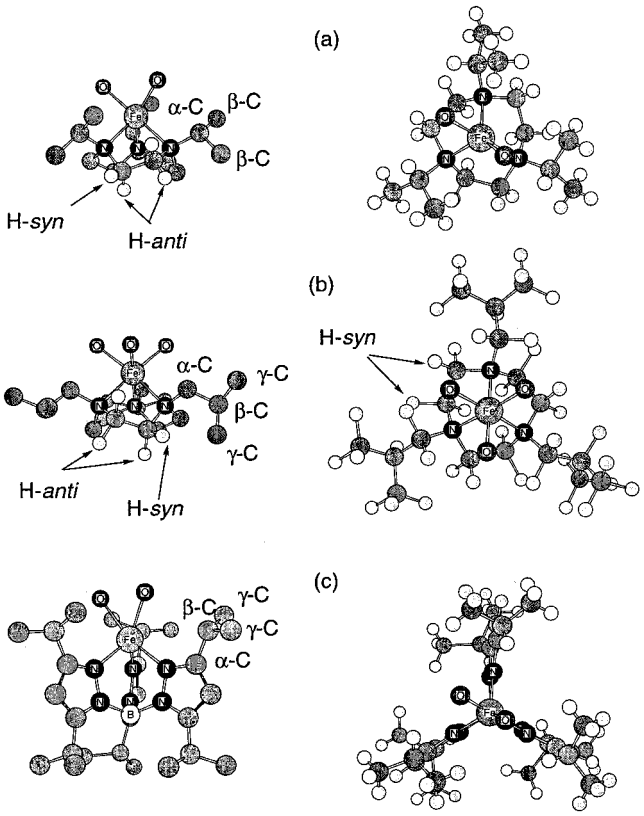

Figure 5. Chem 3D views showing the Fe coordination environments in (a) $\lambda\lambda\lambda$-Fe(*i*-Pr_3tacn)$(CF_3SO_3)_2$ (**2**), (b) $\delta\delta\delta$-Fe(*i*-Bu_3tacn)$(H_2O)(CF_3SO_3)_2$ (**7**), and (c) $FeTp^{i-Pr2}(O_2CCMe_3)$. Left view: parallel to the plane of nitrogen atoms. Right view: down the pseudo-C_3 axis. Selected hydrogen atoms have been omitted for clarity.

$= 160.5(4)°$) because of an interaction with a triflate oxygen from a neighboring complex (C2N···O3′ = 3.24 Å).

Fe(*i*-Bu_3tacn)$(H_2O)(CF_3SO_3)_2$ (7). The structure of the neutral complex **7** is depicted in Figure 4 and shows a six-coordinate iron(II) cation surrounded in a facial fashion by the three nitrogen atoms of the *i*-Bu_3tacn ligand, two monodentate triflate anions, and a water molecule. The coordination sphere about the iron(II) center is an approximate octahedron. The iron amine bond lengths (Table 3) are characteristic of high-spin iron(II), and the intraligand N−Fe−N bond angles average 81.5° to accommodate the five-membered chelate rings. The aqua ligand is hydrogen-bonded to the two triflates bound to a neighboring molecule, as indicated by the O1···O4A and O1···O7A distances of 2.712 and 2.607 Å, respectively. The triflate oxygen atoms O4 and O7 are also hydrogen bonded to a water molecule, as required by the inversion symmetry of **7**, leading to a hydrogen-bonded iron dimer in which the Fe···Fe distance is 6.044 Å.

A comparison of iron(II) complexes of *i*-Pr_3tacn, *i*-Bu_3tacn, and Tp^{i-Pr2} ligands is provided in Figure 5. It is not only the size of the isopropyl and isobutyl groups that result in five- and six-coordinate metals but also the orientation of these groups relative to the ring and metal. The size and conformation of the macrocycles in **2** and **7** are essentially identical. When the three nitrogens of each ring are superimposed (average deviation, 0.02(1) Å), the average deviation of the ring carbons is only 0.04(2) Å. The α-carbons on the substituents deviate by only 0.10(5) Å, and the deviations of the *β*-carbons range from 0.18 to 0.44 Å. The metal in the six-coordinate complexes **6** and **7** lies 1.45 and 1.46 Å, respectively, from the plane of the three amines but only 1.39 Å from the plane in the five-coordinate complex **2**. The five-coordinate Co lies only 1.31 Å from the N_3 plane in **3**. The metal lies between 1.25 and 1.38 Å from the N_3 plane in Cu complexes with *i*-Pr_3tacn[31,32] and 1.22 Å in the only Zn complex of this ligand.[27] The only six-coordinate complexes with *i*-Pr_3tacn that have been structurally characterized are those of Mo and W with sterically nondemanding ligands.[20−23] The Mo- or W-to-N_3 plane distance varies from 1.65 to 1.77 Å.

The α-carbons define a plane that is closer to the metal, nearly parallel to the N_3 plane, and only 0.66 Å from the plane in **2**, 0.51 Å in **3**, 0.71 Å in **6**, and 0.70 Å in **7**. The average distance of these α-carbons from the metal is 3.11 Å in **2** and 3.06 Å in **6**. The three *β*-carbons are 4.5 Å from the iron and nearly coplanar with the N_3 plane in **6** and **7** (two lie on one side of the N_3 plane, although the last carbon lies on the other side) and, therefore, do not interfere with the metal. However, in **2** there are two types of *β*-carbons. One set (C8, C11, and C14) is distant from the metal (average Fe···C distance, 4.5 Å) and forms a plane 0.27 Å from the N_3 plane. The other set (C9, C12, and C15) is much closer to the metal (3.4 Å) and forms a plane tilted 8.9° from the N_3 plane, but this plane is only 0.22 Å from the iron. These methyl groups constrain the size of the pocket such that only two additional ligands bind to the metal. The *γ*-carbons are at an average distance of 5.4 Å from the iron in **6** and do not interact with it in this conformation.

The coordination chemistry of sterically hindered hydrotris(pyrazolyl)borate ligands has recently been reviewed.[37] In $Fe(Tp^{i-Pr2})(Me_3CCO_2)$,[18] an example of a five-coordinate iron(II) complex of Tp^{i-Pr2}, the α- and *β*-carbons are constrained by the pyrazole rings, and the latter lie in a plane 0.4 Å above, but only 3.61 Å from, the iron. The *γ*-carbons are oriented 3.9−5.1 Å away from the metal. However, this ligand is not as restrictive as a macrocycle and can accommodate six-coordinate iron complexes.[17,18] The conformations of these substituted tacn ligands are observed in stable solid-state lattices. Rotations of the N−α-C bonds of the substituents of *i*-Pr_3tacn and both N−α-C and α-C−*β*-C bonds of *i*-Bu_3tacn in solution will induce even more constraints to the binding pocket than seen in the solid-state structures.

Solution Behavior According to ^{1}H NMR. Protonation of the ligand causes the ring-methylene resonances (time averaged to one signal at 2.6 ppm) to split into two multiplets consistent with C_{3v} symmetry (Figure S1b). A similar spectrum is seen for the $[Zn(i\text{-}Pr_3tacn)]^{2+}$ complex, except the resonances are shifted slightly downfield (Figure S1b). These two salts serve as diamagnetic reference materials for the paramagnetic complexes that exhibit strongly isotropically shifted ^{1}H NMR resonances. The protonated ligand is formed if water is added to CD_3CN solutions of *i*-Pr_3tacn (Figure S2). Very little $[Fe(i\text{-}Pr_3tacn)]^{2+}$ (characterized by resonances at 51.1, 21.6, and −2.3 ppm) is formed if 1.0 equiv of H_2O is present, but a significant amount is evident when only 0.33 equiv of H_2O is added to the *i*-Pr_3tacn solution prior to the addition of 1.0 equiv of $Fe(CF_3SO_3)_2$. However, if Fe(*i*-Pr_3tacn)$(CF_3SO_3)_2$ is dissolved in CD_3CN and an excess of H_2O is then added, there is no formation of $(i\text{-}Pr_3tacnH)^+$, and the isotropically shifted resonances shift only very slightly. Both the proton and the iron(II) have considerable kinetic stability with respect to substitution in acetonitrile when bound to this bulky ligand. The shifted resonances are not observed in acetone-d_6, indicating that the complex behaves quite differently in this solvent.

The paramagnetic ^{1}H NMR spectra can be a useful tool for the analysis of stereochemistry and the detection and charac-

(37) Kitajima, N.; Tolman, W. B. *Prog. Inorg. Chem.* **1995**, *43*, 419−531.

terization of the structural and electronic equilibria that occur in solutions of high-spin Fe(II) and Co(II) complexes.[38] Sharper, better resolved spectra are generally observed for cobalt(II) complexes compared to analogous iron(II) complexes because of the faster relaxation rates and greater dipolar shifts associated with high-spin cobalt(II).[39,40] The spectra of mononuclear and dinuclear iron(II) complexes of tacn and Me_3tacn have been studied in considerable detail.[41,42] A rapid flip of the ring pucker in the five-membered NCH_2CH_2NM rings causes an interconversion of $\lambda\lambda\lambda$ and $\delta\delta\delta$ isomers and effectively equilibrates the environment of the two CH_2 groups (Figure 5). This results in two distinct methylene hydrogens that are syn and anti to the bound metal atom. Complexes with an effective mirror plane perpendicular to the ligand, such as $[Fe_2(OH)(O_2CR)_2(Me_3tacn)_2]^{+}$ [40] or $[Fe(Me_3tacn)L_2X]^{+}$, exhibit eight resonances (six from the three unique CH_2 groups and two from the inequivalent methyls). The ^{1}H NMR spectra of the different paramagnetic complexes are presented in Figures 6 and S2−5.

In deuterated acetonitrile, the ^{1}H NMR spectrum of the high-spin cobalt(II) complex **3** (Figure S3a) consists of resonances of the *i*-Pr_3tacn ligand at 226.7 and 39.9 ppm (methylene proton) and at −68.4 and −33.1 ppm for the CH and methyl protons, respectively. The most striking feature of this spectrum is the effective C_{3v} symmetry of the molecule rather than the lower symmetry associated with the five-coordinate structure observed in the solid state. The fluxional behavior that results in this apparent higher symmetry also broadens the resonances so that the resulting spectrum provides less information about the solution structure of cobalt(II) complexes of these ligands than we have observed with other ligands.[40] When a noncoordinating solvent was used for **3** ($CDCl_3$, spectrum not shown), the methylene resonances are not observed, and only two very broad peaks are observed at −78.9 and −43.2 ppm, which are assigned to the CH and CH_3 protons, respectively. This may be a result of the triflate anions coordinating more strongly, and the fluxional behavior is slowed sufficiently to broaden the methylene resonances into the baseline. The large difference observed in the isotropic shifts of the syn and anti CH_2 hydrogens is a result of significantly different contact and dipolar interactions with the paramagnetic cobalt(II). If the time-averaged magnetic axis of the complex passes through the Co and the centroid of the macrocycle, there may be a sign reversal of the dipolar shifts on switching from the anti to the syn methylene hydrogens and the alkyl substituents on the nitrogen. This results in downfield shift of the anti methylene hydrogens and an upfield contribution to the isotropic shifts of the other hydrogens.

The solution behavior of the cobalt(II) *i*-Bu_3tacn complex **8** in CD_3CN is similar to its *i*-Pr_3tacn analogue **3**, showing five well-separated but very broad resonances (Figure S3b). The resonances of the protons on the macrocyclic ring are significantly downfield shifted (191.2 and 39.5 ppm), whereas the resonances for the CH_3 protons (−10.4 ppm on γ-C), the CH protons (−19.3 ppm on β−C), and the CH_2 protons (−47.8 ppm on α-C) of the isobutyl groups are shifted upfield. The pattern of shifts of protons on the α- and β-carbon atoms (−49.1 and −22.7 ppm) are similar to the analogous protons in **3**, although the magnitude is not as great. The greater isotropic shifts observed for the five-coordinate complex are consistent with the tighter binding of the metal to the macrocycle observed in the solid-state structures of **3** compared to **2**, **6**, and **7**. Dipolar shifts are large in cobalt(II) complexes and sensitive to small changes in distance of the protons from the paramagnetic center.[39] The smaller isotropic shifts of the more distant methyl protons in **8** are a result of the attenuation of the contact and dipolar shifts with distance from the paramagnetic center.

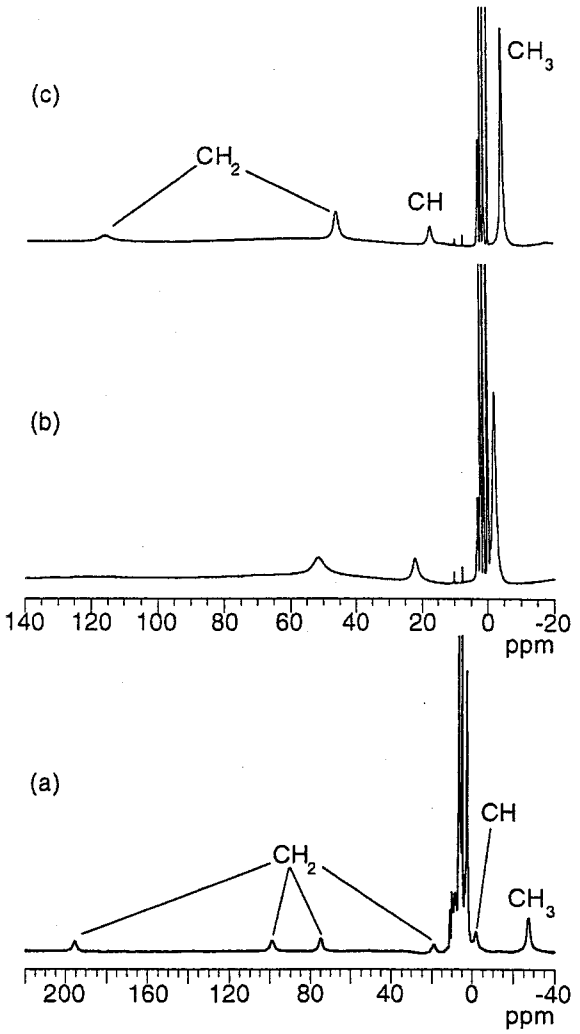

Figure 6. ^{1}H NMR spectra of the Fe(*i*-Pr_3tacn)$(CF_3SO_3)_2$ complex (**2**) (a) in CD_2Cl_2 at 22 °C, (b) in CD_3CN at 22 °C, and (c) in CD_3CN at 78 °C.

The ^{1}H NMR spectrum of the iron complex **2** in CD_2Cl_2 exhibits six isotropically shifted resonances between 200 and −30 ppm in addition to those in the diamagnetic region (Figure 6a). These peaks are accounted for by the presence of a paramagnetic *i*-Pr_3tacn complex and one or more diamagnetic species in solution. The large paramagnetic shifts are typical of high-spin iron(II) complexes, and all the resonances expected for an *i*-Pr_3tacn complex with effective C_3 symmetry are observed. Despite the asymmetry in the solid-state structure of Fe(*i*-Pr_3tacn)$(CF_3SO_3)_2$, only one set of ligand resonances appeared in its NMR spectrum. However, the four resonances for the CH_2 backbone protons (195.6, 98.6, 74.3, and 17.8 ppm) indicate that the $\lambda\lambda\lambda \leftrightarrow \delta\delta\delta$ interconversion in this solvent is slow relative to the NMR time scale. The average C_3 symmetry is therefore not a result of the conformational exchange of the macrocycle but, rather, of the coordinated triflates. Although

(38) Holm, R. H.; Hawkins, C. J.. In *NMR of Paramagnetic Molecules*; LaMar, G. N., Horrocks, W. D., Holm, R. H., Eds.; Academic Press: New York, 1973; Chapter 7.
(39) Bertini, I.; Luchinat, C. In *NMR of Paramagnetic Molecules in Biological Systems*, 3rd ed.; Benjamin/Cummings: Menlo Park, CA, 1986; Chapters 7 and 9.
(40) Lachicotte, R.; Kitaygorodskiy, A.; Hagen, K. S. *J. Am. Chem. Soc.* **1993**, *115*, 8883−8884.
(41) Hagen, K. S.; Diebold, A. Manuscript in preparation.
(42) Blakesley, D.; Payne, S. C.; Hagen, K. S. *Inorg. Chem.* **2000**, *39*, 1979−1989.

dipolar contributions to the isotropic shifts of iron(II) complexes are considerably smaller than observed with cobalt(II) complexes, the upfield resonances at −2.9 and −28.3 ppm are likely to be those of the CH and CH_3 groups, respectively.

The ^{1}H NMR spectrum of complex **2** (Figure 6b) dissolved in CD_3CN is somewhat different from that of **2** dissolved in CD_2Cl_2. Only three relatively broad resonances corresponding to the methylene protons (51.1 ppm), the CH protons (21.6 ppm), and the methyl protons (−2.3 ppm) are observed at room temperature. The second peak for the methylene protons completely broadens into the baseline. The fluxional behavior is sufficiently rapid at 78 °C so that the resonance for these other hydrogens is sharpened and appears at 116 ppm (Figure 6c). The shifts of the methylene resonances are between those of the corresponding resonances observed in CD_2Cl_2, which is consistent with a rapid $\lambda\lambda\lambda \leftrightarrow \delta\delta\delta$ interconversion in CD_3CN. At −25 °C, the resonances broaden even more, and new resonances appear, but the system has not slowed sufficiently to lock in a recognizable lower symmetry structure. This is similar to the dynamic behavior observed for iron(II) complexes with the tetradentate ligand, tris(2-pyridylmethyl)amine.[43,44] The different dynamic behavior observed in CD_3CN versus CD_2Cl_2 is likely to be caused by the substitution of the two triflate anions with coordinated acetonitrile ligands from the bulk solvent. The large paramagnetic shifts as well as the lack of color are typical for a high-spin iron(II) complex. Purple low-spin complexes that exhibit a low-spin/high-spin crossover behavior have been observed with tacn or Me_3tacn ligands in acetonitrile solution.[41,42]

The solution behaviors of *i*-Bu_3tacn complexes **6** and **7** are very similar despite the different coordination in the solid state, indicating that in a given solvent, the species in solution undergo similar fluxional behavior. In $(CD_3)_2CO$ at room temperature, four well-separated peaks are observed with the methylene backbone protons appearing as two relatively broad peaks at 133.3 and 42.9 ppm while the CH_3 protons and the CH protons are upfield shifted at −4.5 and −13.2 ppm, respectively. The isobutyl methylene proton resonance is completely broadened to be undetected even at elevated temperatures. The ^{1}H NMR spectrum of complex **6** in CD_3CN (Figure S3a) exhibits a similar pattern, with only resonances corresponding to the methylene backbone protons (113.5 and 48.3 ppm), the methyl protons (−1.8 ppm), and the CH protons (−8.1 ppm). The isobutyl methylene protons can only be observed at higher temperatures with a peak growing at 19.5 ppm at 78 °C (Figure S3b). All the resonances in both **2** and **6** become sharper, and the magnitude of the isotropic shifts decreases with increasing temperature.

Electronic Absorption Spectroscopy. Cobalt(II) has been widely used in coordination chemistry because cobalt(II) complexes have electronic spectra indicative of their stereochemistry. The spectra of complexes **3** and **4** present identical features (bands at 470, 525, and 652 nm for **3** and at 464, 530, and 671 nm for **4** in Figure S5), indicating that the stereochemistries around the cobalt(II) in solution are likely the same. These bands in the visible region are consistent with spin-allowed d−d transitions for a five-coordinate trigonal bipyramidal cobalt(II) ion.[45] In contrast, six-coordinate octahedral cobalt(II) species exhibit three transitions, and in general, two principal regions of absorption are observed. For complex **8**, a band near 1027 nm of 8 M^{-1} cm^{-1} intensity can be assigned to the $^4T_{2g} \rightarrow {}^4T_{1g}$ transition. In addition, a second band assigned to the $^4T_{1g}(P) \rightarrow {}^4T_{1g}$ is seen in the visible region near 470 nm with 32 M^{-1} cm^{-1} intensity, while the shoulder near 526 nm corresponds to the transition to $^4A_{2g}$. This difference in the absorption spectra is further evidence that steric interactions involving the bulky substituents of the macrocycles in solution result in complexes with different stereochemistries around the metal ion.

Conclusion

This work provides direct experimental support that the two sterically hindered macrocycles 1,4,7-triisopropyl-1,4,7-triazacyclononane and 1,4,7-triisobutyl-1,4,7-triazacyclononane coordinate well as tridentate ligands to divalent transition metals (Fe, Co, and Zn). This reaction system affords a number of different and novel species in the solid state and solution, depending on the solvent used. The solid-state structures of four complexes (**2**, **3**, **6**, and **7**) have been firmly established by X-ray crystallography to possess C_1 symmetry. In contrast, in solution all the complexes exhibit a dynamic behavior that averages the environments of the ligand on the NMR time scale. The solid-state and solution studies have demonstrated that steric interactions involving the bulky substituents of the macrocycles result in different stereochemistries around the metal center. Complexes containing the *i*-Pr_3tacn ligand contain five-coordinate metals, while six-coordinate complexes are isolated with *i*-Bu_3tacn. Additionally, these two ligands form colorless high-spin iron(II) complexes in acetonitrile solution, although the tacn or Me_3tacn macrocycles form low-spin complexes or exhibit a spin equilibrium behavior in solution. Because a monoprotonated complex can be easily formed with these ligands, the solvent used for the synthesis of transition metal complexes plays a fundamental role. To avoid the presence of ionizable protons in the reaction mixture, we have used dry acetonitrile to form the LM fragment. Once this kinetically and thermodynamically stable fragment has formed, the addition of protic solvent (methanol or water) does not result in ligand dissociation and formation of the inert, protonated ligand. We believe that this new series of complexes provides us with useful starting material in modeling the active sites of non-heme metalloproteins and in providing precedence for postulated intermediates during the oxidation process. This is the focus of ongoing efforts in our laboratory.

Acknowledgment. This work was supported by grants from the National Institutes of Health (GM 46506 and S10 RR07323).

Supporting Information Available: ^{1}H NMR spectra of (*i*-Pr_3tacnH^+)(ClO_4^-), **3**, **6**, and **8** in CD_3CN at room temperature (Figures S1−4), electronic absorption spectra of complexes **3** and **8** in CH_3CN (Figure S5), and diagrams displaying the full atom-labeling scheme for complexes **2**, **3**, **6**, and **7** (Figures S6−9). This material is available free of charge via the Internet at http://pubs.acs.org.

IC000456H

(43) Menage, S.; Zang, Y.; Hendrich, M. P.; Que, L. *J. Am. Chem. Soc.* **1992**, *114*, 7786−7792.
(44) Diebold, A.; Hagen, K. S. *Inorg. Chem.* **1998**, *37*, 215−223.
(45) Lever, A. B. P. In *Inorganic Electronic Spectroscopy*, 2nd ed.; Elsevier: New York, 1984; pp 376−611.